Structural elucidation of metabolites of tanshinone I and its analogue dihydrotanshinone I in rats by HPLC–ESI-MS^n

Mingming Wang, Haixue Dai, Xiaorong Li, Yuhang Li, Lijuan Wang, Ming Xue*

Department of Pharmacology, School of Chemical Biology & Pharmaceutical Sciences, Capital Medical University, Beijing 100069, PR China

ARTICLE INFO

ABSTRACT

Tanshinone I and its analogue dihydrotanshinone I are the major active components isolated from *Salvia miltiorrhiza* Bunge and *Salvia Przewalskii* Maxim. These compounds have been found to possess significant antibacterial, anti-dermatophytic, antioxidant, anti-inflammatory and anticancer activities. Fifteen phase I metabolites and two phase II metabolites of tanshinone I and dihydrotanshinone I in rat bile were elucidated and identified by a sensitive HPLC–ESI-MS^n method. The molecular structures of the metabolites are presented on the basis of the characteristics of their precursor ions, product ions and chromatographic retention times. The results indicate that the phase I metabolites are biotransformed through four main pathways: dehydrogenation, hydroxylation, furan ring cleavage and oxidation metabolism. Phase II metabolites were mainly identified as the sulfated conjugates which showed a characteristic neutral loss of 80 Da. The biotransformed pathways of tanshinone I and dihydrotanshinone I were proposed on the basis of the investigation.

1. Introduction

Traditional Chinese medicine (TCM) has gained ever-increasing prevalence in the world due to the therapeutic benefits against particular diseases and these benefits are mostly ascribed to the active metabolites present in the natural medicines [1]. Therefore, the investigation of the active metabolites present in TCMs and the preparations of these active ingredients are very significant in the elucidation of their therapeutic mechanisms.

The root of *Salvia miltiorrhiza* Bunge (SMB) named Danshen in China and *Salvia Przewalskii* Maxim (SPM) as the analogue of Danshen, has been used extensively for at least one thousand years as a treatment of coronary heart diseases, particularly angina pectoris and myocardial infarction [2,3]. According to the chemical structures and pharmacological activities, the major constituents in SMB and SPM are classified into two groups: (i) phenolic acid components such as danshensu (3,4-dihydroxyphenyl lactic acid), propanoid acid, protocatechuic aldehyde and salvianolic acid B and (ii) tanshinones such as tanshinone I, dihydrotanshinone I, tanshinone IIA and cryptotanshinone. The latter group belongs to the diterpenes with an abietane-type skeleton containing a 1,2- or 1,4-quinone in the C-ring [4]. Tanshinone I and its analogue dihydrotanshinone I, which represent the mainly active components isolated from the root of SMB and SPM, have attracted of the attention of chemists and clinicians due to

their versatile pharmacological activities including antibacterial and anti-dermatophytic [5–7], anti-inflammatory [8,9], anticancer [10,11] and hepatic-protection [12,13] activities. Research on tanshinone I and dihydrotanshinone I has mainly focused on the isolation, quantification and pharmacological activities [14–17] with only a few paper characterizing the structural elucidation of the metabolites of tanshinone I and dihydrotanshinone I by liquid chromatography–electrospray ionization tandem mass spectrometry (LC–ESI-MS^n) [18–20]. In this paper, fifteen phase I and two phase II metabolites of tanshinone I and dihydrotanshinone I were simultaneously elucidated and identified by a LC–ESI-MS^n method and the fifteen newly discovered metabolites were presented in rat bile for the first time. The structures of these metabolites were characterized on the basis of their precursor ions, product ions and HPLC retention times. Finally, the biotransformation pathways of tanshinone I and dihydrotanshinone I in rats were elucidated on the basis of an in vivo metabolic study. This investigation should aid further understanding of the metabolic mechanism and intermediate processes of these tanshinone compounds. The data provides important information for predicting the metabolic stability, the development of novel drugs as well as lead compounds, and the better use of TCM containing tanshinones in the clinical setting.

2. Experimental

2.1. Chemicals and reagents

Tanshinone I (1,6-dimethyl-phenanthro[1,2-b]furan-10,11-dione, TS, mw = 276) and dihydrotanshinone I (1,1-dimethyl-

---

* Corresponding author. Tel.: +86 10 83911520; fax: +86 10 83911520.
  E-mail address: xuem@ccmu.edu.cn (M. Xue).

1,2-dihydrophenanthro[1,2-b]furan-10,11-dione, DT, mw = 278) were both obtained from our laboratory. Both Tanshinone I and dihydrotanshinone I were isolated and purified from the root of *S. miltiorrhiza* Bunge and *S. Przewalskii* Maxim, and identified as pure compounds from melting point, IR, UV, MS, NMR analysis and comparison with the standard compounds. The purities of tanshinone I and dihydrotanshinone I were both >99% [5]. The standard compounds, tanshinone I and dihydrotanshinone I were purchased from the National Institute for the Control of Pharmaceutical and Biological Products (Beijing, China). HPLC grade methanol was used and purchased from Fisher Scientific Products (Fair Lawn, NJ, USA). Water was triply distilled. Ethyl acetate and other reagents and solvents were all of analytical grade.

2.2. Apparatus and analytical conditions

The LC–ESI-MS system consisted of a HPLC system (Series 1100, Agilent technology, Palo Alto, CA, USA) including a HP 1100 G1312A binary pump, G1379A vacuum degasser and G1313A autosampler that was coupled to a Finnigan LCQ Deca XP ion trap mass spectrometer (ITMS) equipped with an electrospray ion source (ESI) (Thermo Finnigan, San Jose CA, USA). The LC–ESI-MS system was controlled by the Xcalibur® (version 1.3) software.

Separation of tanshinone I and dihydrotanshinone I and their metabolites was achieved on a Betamax Acid C_{18} reversed-phase LC column (150 × 2.1 mm, i.d., 5 μm; Thermo Electron, CA, USA) at a flow rate of 0.2 ml/min at ambient temperature. The mobile phase was composed of methanol and water (75:25, v/v) and 5 μl samples were introduced into the LC–ESI-MS system for both the organic and aqueous metabolites. The flow from the column (unsplit) was directed into the mass spectrometer with a minimal amount of PEEK tubing (Upchurch, Oak Harbor WA, USA). The run time of the samples was 20 min.

HPLC/MS^n analysis was performed with an Agilent 1100 Series and Finnigan LCQ Deca XP ion trap mass spectrometer with Xcalibur® 1.3 controlling software. The experiments utilized electrospray ionization coupled with collision induced dissociation (CID) in the positive and/or the negative ion mode. The ESI-MS was operated at the sheath flow rate of 413.4 kPa; capillary temperature of 350 °C; capillary voltage of 12 V and the electrospray voltage ranged from +3.5 to +5 kV. Ultra-high purity helium was used as the collision gas for the collision induced dissociation (CID) experiments. Nitrogen was used as both the drying gas and the nebulizing gas, which was set at 172.3 and 34.5 kPa for the sheath and auxiliary gases, respectively. The MS^n product ion spectra were produced by collision induced dissociation of the protonated molecular [M+H]$^+$ ion of each analyte at their respective HPLC retention times. Collision energy for TS, DT and their metabolites was dependent on the different compounds from 30 to 40% with an isolation width of 1.0 Da and an activation time of 30 ms. In each separate analysis, the data-dependent MS–MS scanning feature of the ion trap was used to ensure comprehensive MS–MS fragment information of the metabolites. The ion spray interface and mass spectrometric parameters were optimized to obtain maximum sensitivity at the unit resolution. The *m/z* values of the parent compounds and the predicted metabolites were put into the parent mass list so that the data-dependent MS^n analysis was preferentially performed on these ions. The quasi-molecular ions of the most abundant endogenous compounds were put in an exclusion list to prevent their data-dependent acquisition.

2.3. Sample preparation

All studies on animals were in accordance with the guidelines of the Committee on the Care and Use of Laboratory Animals of China. Healthy Sprague–Dawley (SD) rats were obtained from the Animals Center of the Capital Medical University in China (CCMU, China). Male SD rats (210–250 g, n = 6) were fasted overnight and water was available ad libitum before use. The rats were anesthetized and fixed on a wooden plate. An abdominal incision was made and the rat bile duct was cannulated with PE-10 tubing (0.08 cm, i.d., Becton Dickinson, USA) for collection of the bile samples. Tanshinone I and dihydrotanshinone I was dissolved in normal saline coupled with 1% Tween-80 to give a concentration of 5 mg/ml for the compounds. The drug solution was filtered using a 0.22 μm filter. A single dose of 25 mg/kg tanshinone I or dihydrotanshinone I was intravenously administered to the rats via the caudal vein and the same volume of 1% Tween-80 without tanshinone I or dihydrotanshinone I was administered as the negative control. Three rats were sorted to a group for each compound. A heating lamp was used for maintaining the rat body temperatures during the experimental procedures. Bile samples were collected for 12 h and all the samples were immediately stored at −80 °C until extraction and analysis.

Three-fold volume of ethyl acetate was added to the bile samples, vortexed for 2 min and centrifuged at 3500 × g for 15 min. The supernatants were extracted three times using ethyl acetate. The upper organic layers were then collected and combined and evaporated to dryness under a stream of nitrogen flow at 40 °C. The lower aqueous layers were treated with methanol for protein precipitation and then lyophilized. The two phase dried residue samples containing metabolites were re-dissolved in 200 μl of methanol followed by filtration with 0.22 μm for LC–ESI-MS^n analysis.

3. Results and discussion

3.1. Mass fragmental analysis of tanshinone I and dihydrotanshinone I

Drug metabolism is the drug structural modification by the in vivo or in vitro enzymatic systems. The parent compounds and their metabolites always possess the great similarity in the chemical structures, therefore, the first step of our investigation involved the characterization of the mass spectrometric fragmentation behaviors of the parent drugs. The mass spectral patterns of the parent compounds served as the templates in elucidation of the structures of the proposed metabolites because the parent compound undergoes extensive and well defined fragmentation under MS–MS conditions and the characteristic product ions and fragmentation rules of the parent drugs could provide the valuable information for extrapolating the structures of the metabolites.

Before characterizing the metabolites of tanshinone I in rats, a full scan mass spectrum of tanshinone I, which showed a protonated molecular ion of *m/z* 277, was analyzed in detail using the optimized chromatographic and mass spectrometry conditions. The CID analysis of the ESI-MS^n product ion spectra of the protonated molecular ion of *m/z* 277 is presented in Table 1 . Fragmentation of the protonated molecular ion of tanshinone I in an ion trap yielded six main product ions at *m/z* 259, 249, 231, 221 and 193. The product ion at *m/z* 259 was formed by the loss of H_2O from the parent molecular ion. The most abundant product ion was *m/z* 249, which was 28 Da less than tanshinone I and was formed by the loss of a CO fragment. The product ion at *m/z* 231 existed in the MS^3 spectra of ions at *m/z* 259 and 249, and the product ion *m/z* 193 was found in both the MS^3 spectrum with an *m/z* 249 and in the MS^4 spectrum with an *m/z* 221. It could be inferred that the ions at *m/z* 249 and 193 were a pair of characteristic product ions of tanshinone I and this ion pair was used for structural elucidation of these metabolites. The molecular structure of tanshinone I and its suggested fragmentation pathway are presented in Fig. 1. The

Table 1
Chromatographic retention times and mass spectrometric data of tanshinone I, dihydrotanshinone I and their phase I metabolites found in rats.

Parent ion	Metabolites	Precursor ion	Retention time (min)	Data-dependent MS^n data (% base peak)
DT	DT	[M+H]+ 279	9.37	MS^2[279]:279(1),261(100),251(3),237(3),235(1),233(9),223(1),215(1),209(2),205(1),169(1) MS^3[279 → 205]:205(100),190(12) MS^3[279 → 209]:209(52),193(3),181(100),166(4) MS^3[279 → 233]:233(48),218(10),215(4),205(100),190(2) MS^3[279 → 251]:251(23),233(9),223(100),209(13),169(34) MS^3[279 → 261]:261(9),233(100),217(1),215(5),205(7),190(1),169(1) MS^4[279 → 237 → 209]:209(28),181(100) MS^4[279 → 261 → 233]:233(67),205(77),195(48),169(100) MS^4[279 → 251 → 223]:223(21),205(5),195(20),169(100)
TS	TS	[M+H]+ 277	14.71	MS^2[277]:277(1)259(5),249(100),235(1),231(12),221(5),207(1),193(1),178(1),169(1) MS^3[277 → 259]:259(100),231(23),203(6) MS^3[277 → 249]:249(100),234(3),231(4),221(31),207(1),206(1),203(2),193(15),178(1),169(4) MS^3[277 → 231]:231(77),203(100) MS^3[277 → 193]:193(100),178(37) MS^4[277 → 249 → 234]:234(100),206(17) MS^4[277 → 249 → 231]:231(72),203(100) MS^4[277 → 249 → 221]:221(59),206(7),203(2),193(100),178(3) MS^5[277 → 249 → 221 → 193]:193(100),178(53)
DT	M1	[M+H]+ 295	8.97	MS^2[295]:295(20),280(13),277(100),267(13),259(2),253(5),249(30),239(2),235(5),231(3),225(25) MS^3[295 → 249]:249(22),234(60),221(100),193(8) MS^3[295 → 277]:277(71),262(22),259(3),249(100),235(13),233(4),231(10),219(3),207(3) MS^4[295 → 249 → 234]:234(80),217(61),206(100) MS^4[295 → 277 → 249]:249(40),234(100),221(10),206(63) MS^5[295 → 277 → 249 → 234]:234(100)
DT	M2	[M+H]+ 295	16.47	MS^2[295]:280(1),277(100),267(1),266(1),259(1),253(2),249(10),235(2),231(1),225(1) MS^3[295 → 249]:249(22),234(60),221(100),193(8) MS^3[295 → 277]:277(52),262(14),259(4),249(100),235(3),234(3),231(6),221(3),206(1),195(1) MS^4[295 → 249 → 234]:234(8),219(14),206(100) MS^4[295 → 277 → 249]:249(78),234(48),231(2),221(100),219(4),207(2),206(40),193(5) MS^5[295 → 277 → 249 → 234]:234(74),219(21),206(100),205(9),191(8)
DT	M3	[M+H]+ 311	6.71	MS^2[311]:311(29),293(70),281(13),275(100),269(12),265(4),263(4),239(9),226(13) MS^3[311 → 275]:275(6),247(100),189(8) MS^3[311 → 293]:311(16),293(11),275(100),265(27),247(36) MS^4[311 → 275 → 247]:219(100),204(62) MS^4[311 → 293 → 275]:275(17),247(100) MS^5[311 → 293 → 275 → 247]:247(47),219(100),204(14),190(13)
DT	M4	[M+H]+ 311	9.07	MS^2[311]:311(5),293(100),275(6),251(2),247(2) MS^3[311 → 293]:293(18),275(100),265(35),247(49)
DT	M5	[M+H]+ 251	10.98	MS^2[251]:251(100),233(34),223(52),222(18)
DT	M6	[M+H]+ 269	8.05	MS^2[269]:269(100),254(13),251(20),241(10),240(10),213(5),212(5),199(12)
TS	M7	[M+H]+ 275	12.96	MS^2[275]:275(10),260(13),247(100),232(2),229(2),219(6),193(1) MS^3[275 → 247]:247(56),232(13),219(100),217(3),204(20),193(15)
TS	M8	[M+H]+ 293	6.52	MS^2[293]:293(19),278(6),275(100),251(4),247(33) MS^3[293 → 275]:275(55),247(100),229(8),205(10) MS^4[293 → 275 → 247]:247(71),219(100),204(43)
TS	M9	[M+H]+ 293	14.01	MS^2[293]: 293(11),278(6),275(100),265(10),251(8),247(25),229(4) MS^3[293 → 275]:275(40),260(5),247(100),229(3),193(1) MS^3[293 → 249]:249(69),232(23),219(100),204(34),193(4) MS^4[293 → 275 → 247]:247(37),232(15),219(100),204(37),193(3) MS^4[293 → 249 → 219]:219(100),204(42), MS^5[293 → 275 → 247 → 219]:219(100),204(42),193(1) MS^5[293 → 249 → 219 → 204]:204(100),189(61)
TS/DT	M10	[M+H]+ 309	7.66	MS^2[309]:309(15),291(100),267(62),266(42),249(27) MS^3[309 → 291]:291(5),273(23),263(100),249(32),245(21) MS^3[309 → 267]:267(5),249(100),221(16) MS^4[309 → 291 → 263]:263(7),248(68),235(100),221(32),217(36) MS^4[309 → 267 → 249]:221(100),193(53) MS^5[309 → 267 → 249 → 221]:221(100) MS^5[309 → 291 → 263 → 248]:248(27),205(100) MS^5[309 → 291 → 263 → 235]:235(100),221(72),207(42)
TS	M11	[M+H]+ 249	7.56	MS^2[249]:249(100),234(5),231(6),221(28),203(4) MS^3[249 → 234]:234(98),204(100) MS^3[249 → 221]:193(100)
TS/DT	M12	[M+H]+ 249	17.35	MS^2[249]:249(100),248(10),231(27),221(26),199(6),193(6) MS^3[249 → 221]:221(70),193(100) MS^4[249 → 221 → 193]: 193(87),178(100)

Table 1 (*Continued*)

Parent ion	Metabolites	Precursor ion	Retention time (min)	Data-dependent MS^n data (% base peak)
TS/DT	M13	$[M+H]^+$ 267	7.58	$MS^2[267]$:267(15),249(100),235(8),210(13) $MS^3[267 \rightarrow 249]$:221(100) $MS^4[269 \rightarrow 249 \rightarrow 221]$:193(100)
TS/DT	M14	$[M+H]^+$ 267	13.49	$MS^2[267]$:267(31),252(8),249(100),224(11),210(10) $MS^3[267 \rightarrow 249]$:249(17),221(100),193(10) $MS^4[269 \rightarrow 249 \rightarrow 221]$:221(70),193(100)
TS	M15	$[M+H]^+$ 265	17.47	$MS^2[265]$:265(100),250(28),247(61),237(61),223(33),209(10) $MS^3[265 \rightarrow 247]$:247(51),219(100)

fragmentation mechanism of tanshinone I also helped to elucidate and identify the metabolite structures.

Similarly, the ESI-MS^n product ion spectra of the protonated molecular ion of m/z 279 of dihydrotanshinone I are presented in Table 1. Fragmentation of the protonated molecular ion of dihydrotanshinone I in the ion trap also produced six major product ions at m/z 261, 251, 233, 223, 205 and 195, which were two protons more than that of tanshinone I. The product ions at m/z 261 and 251 were directly formed by the losses of H_2O and CO from the molecular ion at m/z 279, respectively. The product ion at m/z 233 was produced by the loss of CO from the ion m/z 261 or the loss of H_2O from the ion m/z 251. The product ion at m/z 223 was
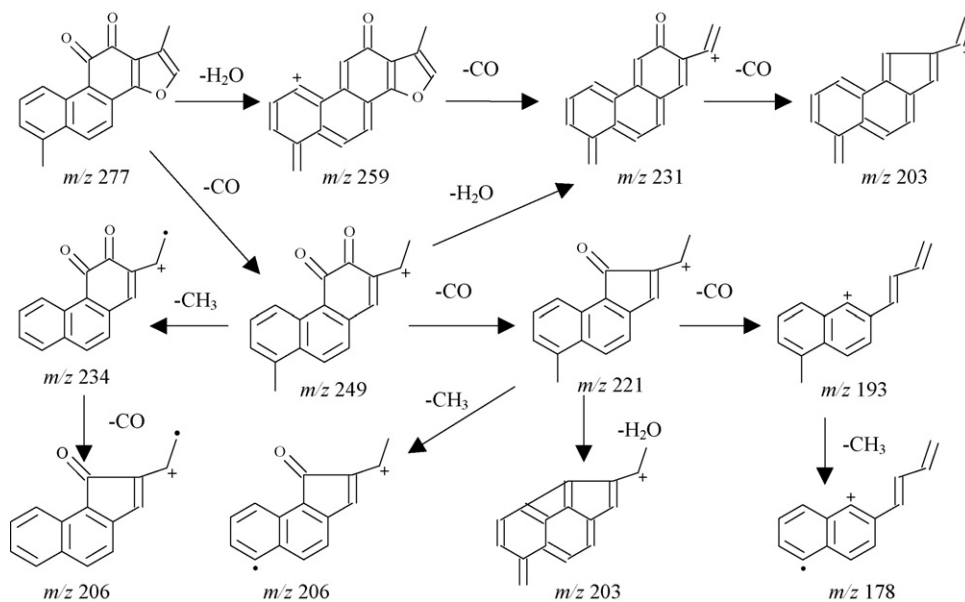

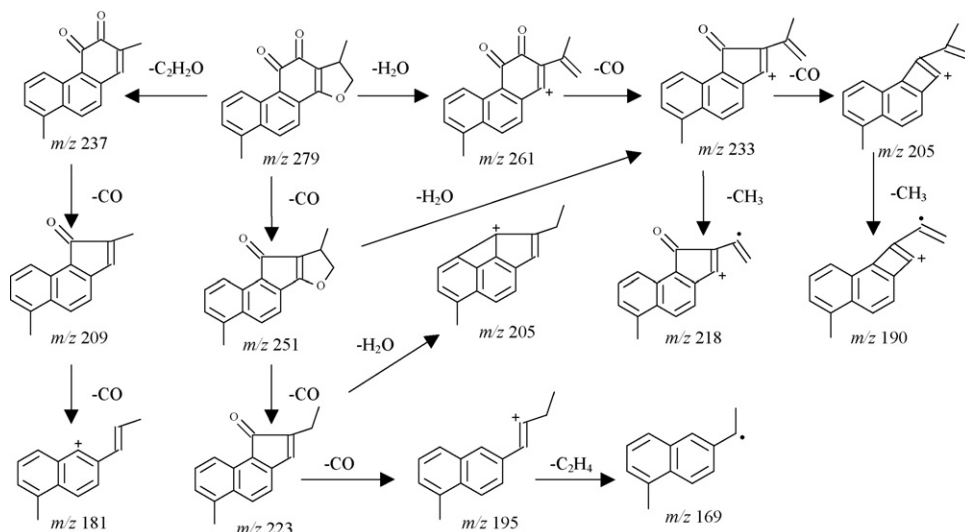**Fig. 1.** The proposed ESI-MS fragmentation pathways of tanshinone I.

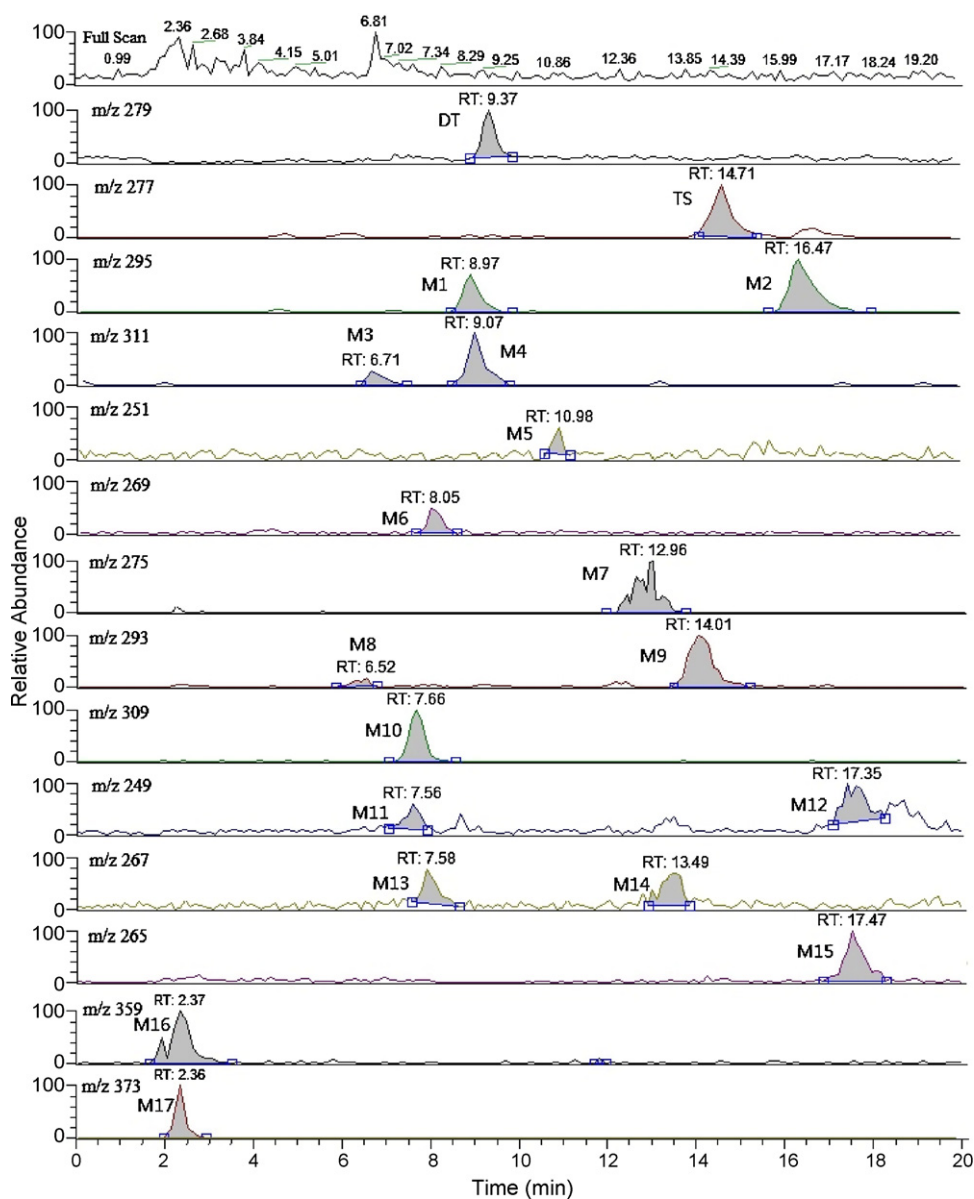**Fig. 2.** The proposed ESI-MS fragmentation pathways of dihydrotanshinone I.

Fig. 3. Total full scan ion and extracted ion chromatograms of tanshinone I, dihydrotanshinone I and their metabolites.

formed via the loss of CO from the ion m/z 251. The fragment ion at m/z 205 existed in the MS^4 spectra of both ions with m/z 233 and at m/z 223 and the ion at m/z 195 was formed by the loss of CO from the ion m/z 223. According to the above analysis, we conclude that the fragment ions at m/z 205 and 195 were the characteristic product ions of dihydrotanshinone I. The molecular structure of dihydrotanshinone I and its suggested fragmentation pathway are presented in Fig. 2. The fragmentation mechanism of dihydrotanshinone I should aid the characterization and identification of these metabolite structures.

3.2. Identification of the metabolites of tanshinone I and dihydrotanshinone I

In vivo metabolism of tanshinone I and dihydrotanshinone I in rats was studied after i.v. administration of the two compounds. Bile samples were collected and extracted with ethyl acetate, respectively. The reconstituted extracts were analyzed by LC/ESI-MS in both positive and negative ion modes. The investigation involved

the characterization of the mass spectral properties of the parent drugs and their metabolites. Using the full scan mass spectral analyses of tanshinone I and its analogue dihydrotanshinone I, characteristic protonated molecular ions of m/z 277 and 279 of the two parent compounds were found. Extracted ion chromatograms of tanshinone I and dihydrotanshinone I as well as their phase I and phase II metabolites in the bile of rats is presented in Fig. 3. The challenge of investigating the in vivo metabolites existed in a relatively low concentration in the biological matrix accompanied by large amounts of endogenous compounds. To reduce the endogenous matrix interference and enhance the level of the trace metabolites, bile samples were extracted three-fold with ethyl acetate and the selective ion monitoring method was used. And the successful initiation of the data-dependent scans for the quasi-molecular ions of the interest compounds was very important for charactering the trace metabolites.

The full scan mass spectra of the metabolite samples were compared with that of the control samples and the parent drugs to identify the proposed metabolites. These compounds were ana-

lyzed by the LC–ESI-MS^n method. Retention times, changes in observed mass (ΔM) and spectral patterns of product ions of the metabolites were compared with that of tanshinone I and dihydrotanshinone I to identify these metabolites and elucidate their structures. Following the determination of the retention times and the mass spectra of the proposed metabolite molecules, the retention time dependent MS–MS scans were programmed to acquire CID data on-line. Structural identification of these metabolites could be hindered by the absence of useful product ions in the MS or MS–MS spectra. Consequently, the pseudo MS^n mass spectra, via in-source fragmentation of molecular ions, were used for more precise structural identification of the metabolites. We revealed that it was essential for the change in many product ions and the structural elucidation of metabolites via a series of comparisons of the product ions of the metabolites with that of the parent drug. Neutral loss scan in MS/MS mode was used to screen the possible phase metabolites such as the glucuronidation with 176 Da and the sulfation with 80 Da. Based on the method described above, we found the fifteen characteristic chromatographic peaks which were the proposed phase I metabolites and two chromatographic peaks as the proposed phase II metabolites in rat bile. The main metabolic mechanism of tanshinone I and dihydrotanshinone I in rats could be described as the dehydrogenation, hydroxylation, furan ring cleavage, oxidation, and the O-sulfation reactions.

Based on the analysis of the MS^n fragments data and on the type of their parent ions, all of the phase I metabolites of tanshinone I and its analog dihydrotanshinone I in rat bile could be divided into three groups: the metabolites exclusively produced by dihydrotanshinone I, the metabolites only formed by tanshinone I and those metabolites that formed from both dihydrotanshinone I and tan-
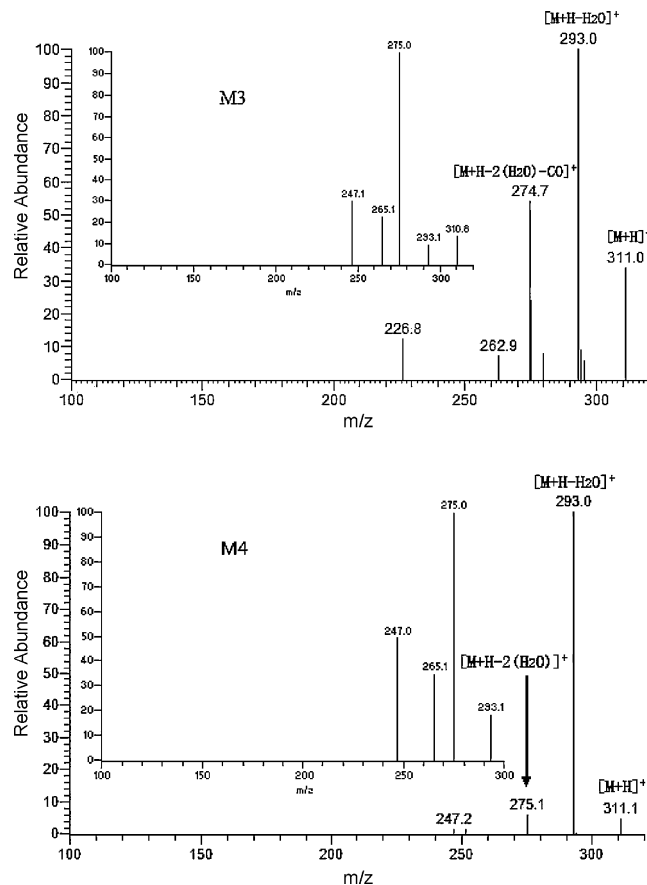

Fig. 5. MS^2, MS^3 spectra of M3 and M4 (M3: MS^2 [311] and MS^3 [311 → 275] spectra; M4: MS^2 [311] and MS^3 [311 → 293] spectra).

shinone I. The mass spectrometric data of protonated product ions of tanshinone I, dihydrotanshinone I and their phase I metabolites along with their HPLC retention times are summarized in Table 1.

3.2.1. Identification of dihydrotanshinone I and tanshinone I in rats

Dihydrotanshinone I and tanshinone I were observed as the protonated molecule [M+H]$^+$ at m/z 279 and 277 with retention times of 9.37 and 14.71 min, respectively. The retention time and the MS^n spectra were the same as those of the standard compound dihydrotanshinone I. DT was confirmed as the unchanged parent drug of dihydrotanshinone I. The retention time and the MS^n spectra were the same as those of the standard compound tanshinone I. TS was confirmed as the unchanged parent drug of tanshinone I and in vivo dihydrotanshinone I was initially biotransformed into tanshinone I [18–20].

3.2.2. Phase I metabolites of dihydrotanshinone I and tanshinone I

M1 and M2, eluted at 8.97 and 16.47 min, both gave rise to protonated quasi-molecules [M+H]$^+$ at m/z 295 and were 16 Da higher than that of dihydrotanshinone I. The product ions spectra of their molecules were shown in Fig. 4. According to the structure of dihydrotanshinone I there are two possible hydroxyl conjugated sites which could form the position isomers of the metabolites with identical molecule weights. The major product ions of M1 and M2 are shown in Table 1. The fragment ion of M1 and M2 at m/z 277 was formed via the elimination of OH and then by the loss of 2H from the parent ion. The product ion at m/z 277 continued to lose CO to form the fragment ion at m/z 249. The fragment ions of the product ion at m/z 277 were similar to those of tanshinone I. According
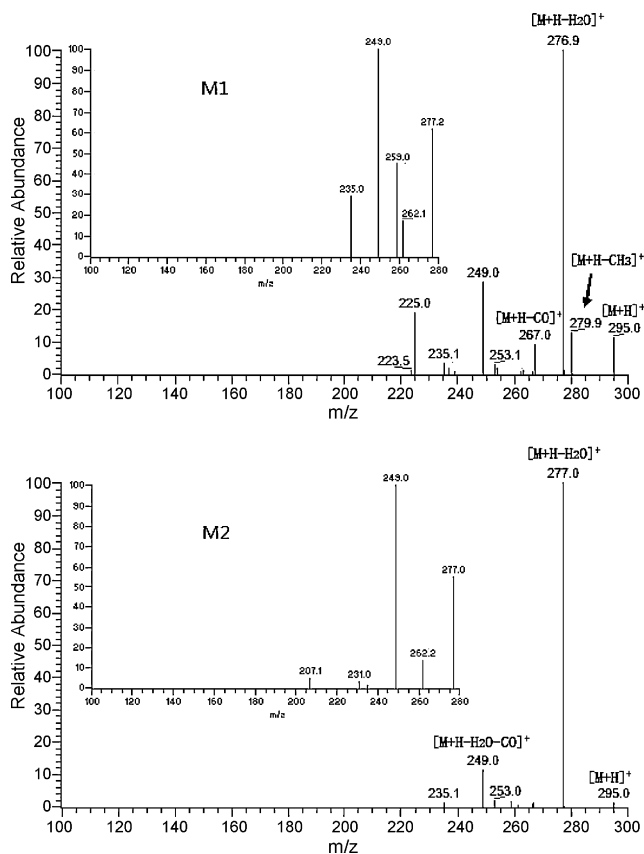

Fig. 4. MS^2, MS^3 spectra of M1 and M2 (M1 and M2: MS^2 [295] and MS^3 [295 → 277] spectra).
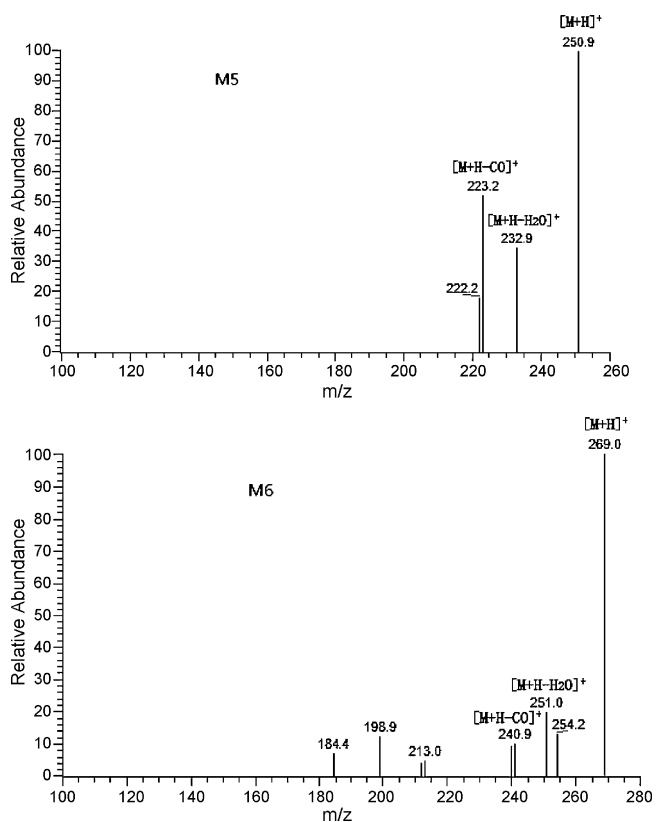
Fig. 6. MS^2 spectra of M5 and M6 (M5: MS^2 [251] spectra; M6: MS^2 [269] spectra).

to the data and the literature [19,20], both M1 and M2 were identified as the monohydroxylated metabolites of dihydrotanshinone I at the different sites. And M1 was presented here for the first time.

M3 and M4, eluted at 6.71 and 9.07 min and gave rise to a protonated quasi-molecular ion [M+H]$^+$ at m/z 311, which was 32 Da higher than that of dihydrotanshinone I. Due to the existing prominent ions at m/z 293 and 275 produced in the MS^n (n = 2–3) spectra, M3 and M4 are therefore proposed as dihydroxylated metabolites of dihydrotanshinone I. Since there were the two types of monohydroxylated metabolites produced from dihydrotanshinone I in rats, the isomers of the dihydroxylated metabolites could potentially exist when these monohydroxylated compounds were further conjugated with a hydroxyl group. M3 was formed by M1 conjugating with a hydroxyl group, and M4 was produced by M2 combining with another hydroxyl group. The product ion spectra of M3 and M4 are shown in Fig. 5. The fragment ions at m/z 293 produced from both M3 and M4 were formed via the loss of OH and 2H from the parent ions, and then the fragment ion at m/z 293 continued to lose H$_2$O to form the fragment ion at m/z 275. Therefore, M3 and M4 were identified as the dihydroxylated metabolites of DT.

M5 gave rise to the protonated molecule [M+H]$^+$ at m/z 251 with a retention time of 10.98 min. This species is 28 Da less than that of dihydrotanshinone I and was produced by furan ring cleavage and the loss of a CO fragment from dihydrotanshinone I. The fragment ions at m/z 233 and 223 were formed through elimination of H$_2$O and CO, respectively (shown in Fig. 6). Consequently, M5 was tentatively elucidated as the metabolite of dihydrotanshinone I by cleavage of the furan ring and loss of CO.

M6, which eluted at 8.05 min, gave rise to the protonated molecule [M+H]$^+$ at m/z 269, which was 18 Da heavier than M5. The fragment ion at m/z 254 was formed via the loss of a CH$_3$ group from the parent ion, the fragment ion at m/z 251 was formed via

the loss of H$_2$O from the parent ion and the fragment ion at m/z 241 was produced through the loss of a neutral CO fragment (shown in Fig. 6). In the light of the above analysis, M6 was tentatively elucidated as the hydroxylated metabolite of M5 at the side chain carbon position. This metabolite was also produced from dihydrotanshinone I by furan ring cleavage. The formation of M5 and M6 from dihydrotanshinone I was similar to that of cryptotanshinone [21].

M7, which eluted at 12.96 min, gave rise to the protonated molecule [M+H]$^+$ at m/z 275 (shown in Fig. 7). The fragment ion at m/z 260 was formed via the loss of a CH$_3$ group from the parent ion, and the product ion at m/z 247 was produced through the elimination of CO from the precursor ion. The daughter ions at m/z 232, 229 and 219 were produced by the loss of CH$_3$, H$_2$O and CO from the fragment ion m/z 247, respectively. The product ions at m/z 204 and 193 were formed by the loss of CH$_3$ and CO from the ion at m/z 219, and the fragment ion at m/z 207 was formed via a type of charge transfer and proton loss from the fragment at m/z 219 (shown in Fig. 7). The proposed ESI-MS fragmentation pathway of M7 is shown in Fig. 8.

M8 and M9, which eluted at 6.52 and 14.01 min, both gave rise to the protonated molecule [M+H]$^+$ at m/z 293 and were 16 Da higher than that of tanshinone I. Both species produced the product ions at m/z at 278 and 275 by the loss of CH$_3$ and H$_2$O, respectively. The daughter ion at m/z 247 was formed by the loss of CO from the ion at m/z 275. According to the similar product ions spectra, we infer that M8 and M9 were the hydroxylated isomers produced from TS. In a similar manner to DT, there could also be two conjugating sites within the tanshinone I skeleton, which could combine with hydroxyl groups at different sites. According to the analysis above and the literature [19,20], M8 and M9 were elucidated as the monohydroxylated metabolites of tanshinone I at the different sites (shown in Fig. 9). And M9 was presented here for the first time.

M10, which eluted at 7.66 min, gave rise to the protonated molecule [M+H]$^+$ at m/z 309, which was 32 Da heavier than tanshinone I. The fragment ion of M10 at m/z 291 was formed via the loss of H$_2$O from the parent ion. The MS^3 product ion spectra of M10 gave a prominent protonated molecule [M+H]$^+$ at m/z 273, which was produced via the loss of neutral H$_2$O from the fragment ion at m/z 291 (shown in Fig. 9). According to the analysis above, M10 represents the dihydroxylated metabolite of TS, which was formed from M8 and/or M9. We could further infer that, first, two hydroxylated isomers of tanshinone I were produced, and then, another hydroxyl group was added to the two isomers to form the dihydroxylated metabolite, M10. Dihydrotanshinone I also existed via a similar metabolic pathway because of the same characteristic structures.

M11 and M12, which eluted at 7.56 and 17.35 min, both gave rise to the protonated quasi-molecule [M+H]$^+$ at m/z 249, which
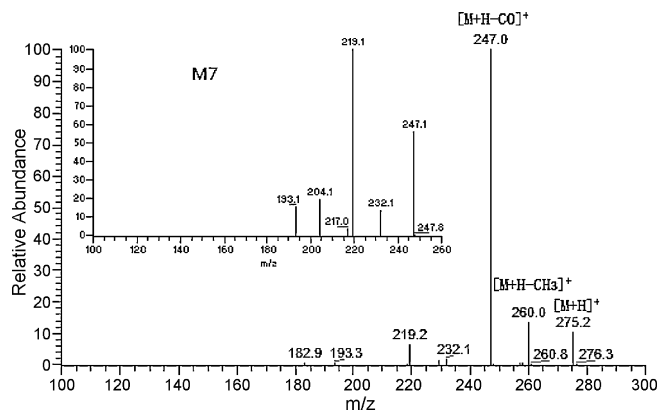

Fig. 7. MS^2, MS^3 spectra (M7: MS^2 [275] and MS^3 [275 → 247] spectra).
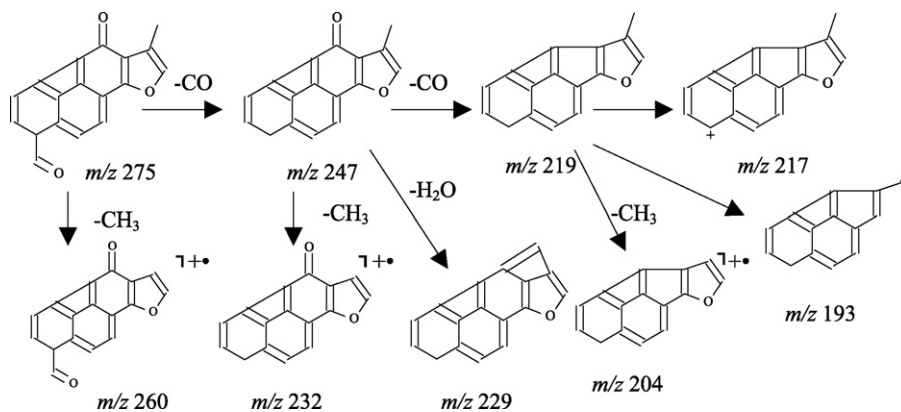
Fig. 8. The proposed ESI-MS fragmentation pathway of M7.

was 28 Da less than tanshinone I and could be produced by the furan ring cleavage and the loss of a CO fragment from tanshinone I. The fragment ions of M11 at m/z 231 and 234 were formed via the loss of H_2O and CH_3 from the parent ion, respectively. The fragment ion of M11 at m/z 221 was produced by the elimination of CO from M11. The fragment ion at m/z 221 fragmented into its daugh-

ter ions at m/z 193 and 203 through the further loss of second CO and H_2O moieties (shown in Fig. 10). The retention time and chromatographic features of M12 were different from that of M11. The fragment ions of M12 at m/z 231 and 234 were formed via the loss of H_2O and CH_3 from the parent ion, respectively. The fragment ion of M12 at m/z 221 was produced by the elimination of CO from the parent ion at m/z 249. The fragment ion at m/z 221 fragmented into its daughter ions at m/z 193 and 178 through the additional loss of CO and H_2O (shown in Fig. 10). The product ion at m/z 178 was also formed by the loss of CH_3 from the precursor ion at m/z 193. According to the above analysis and the mass spectral data, M11 and M12 were the position isomers.

M13 and M14, which eluted at 7.58 and 13.49 min, both gave rise to the protonated molecules $[M+H]^+$ at m/z 267, which were
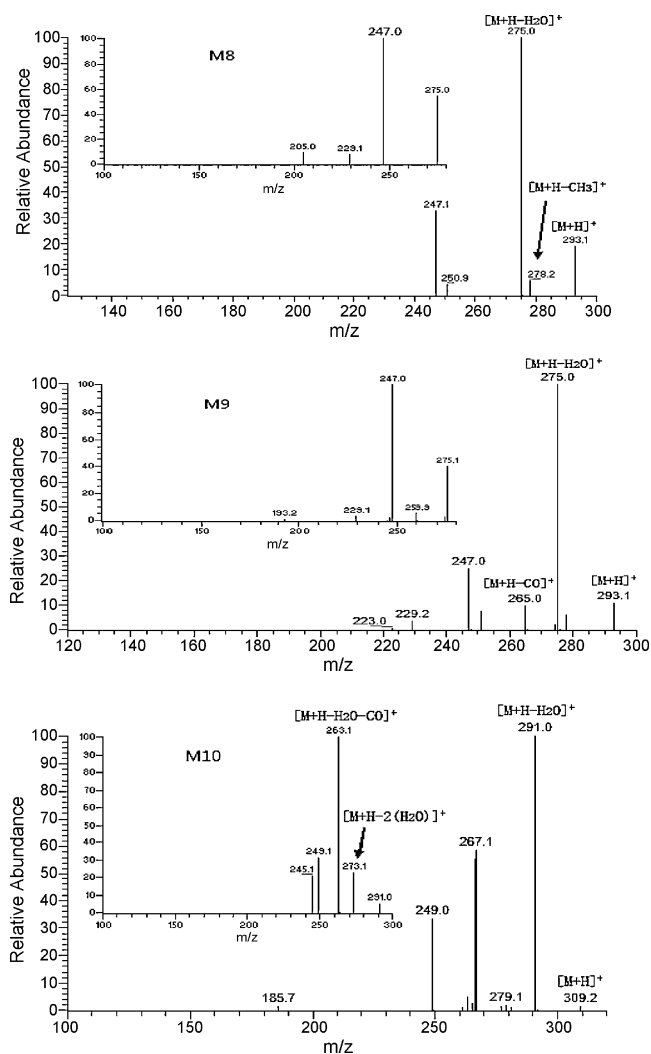

Fig. 9. MS^2, MS^3 spectra of M8, M9 and M10 (M8: MS^2 [293], MS^3 [293 → 275] spectra; M9: MS^2 [293], MS^3 [293 → 275] spectra; M10: MS^2 [309], MS^3 [309 → 291] spectra).
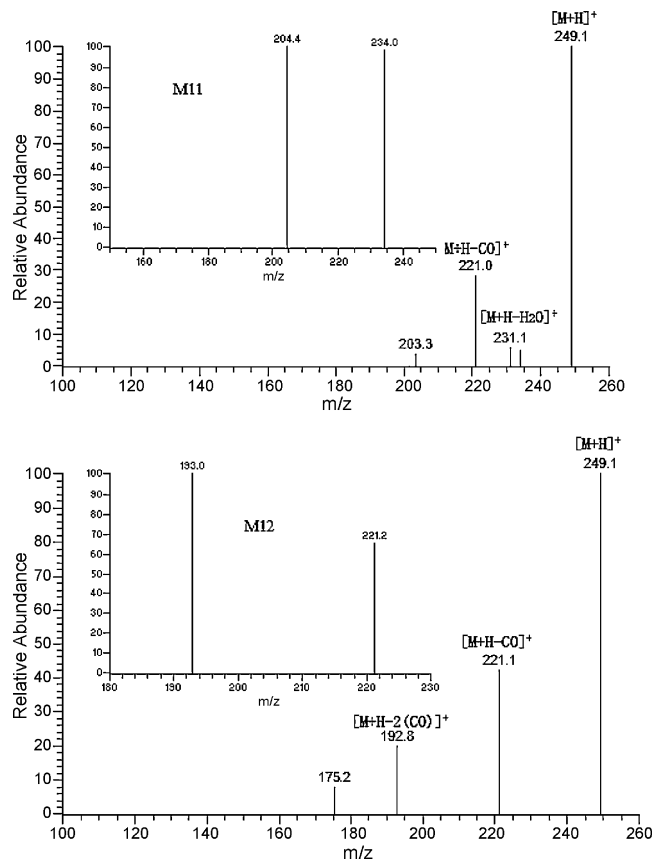
Fig. 10. MS^2, MS^3 spectra of M11 and M12 (M11: MS^2 [249] and MS^3 [249 → 234] spectra; M12: MS^2 [249] and MS^3 [249 → 221] spectra).

Fig. 12. MS^2 spectra of M16 and M17 (M16: MS^2 [359] spectra; M17: MS^2 [373] spectra).
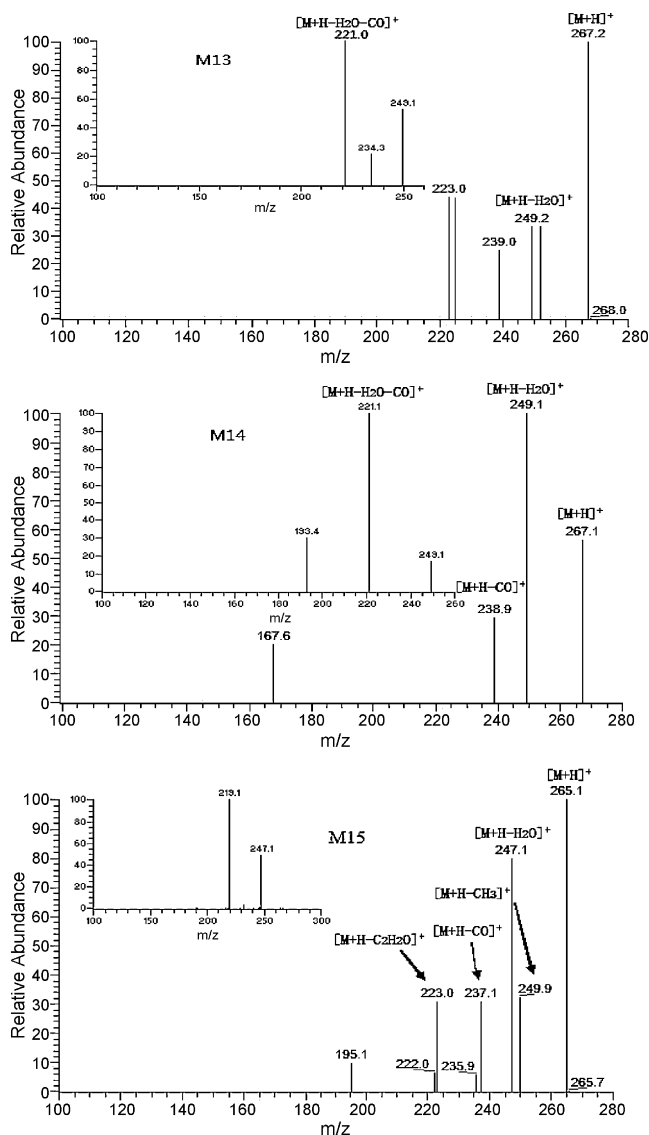
Fig. 11. MS^2, MS^3 spectra of M13, M14 and M15 (M13: MS^2 [267] spectra, MS^3 [267 → 249] spectra; M14: MS^2 [267] spectra, MS^3 [267 → 249] spectra; M15: MS^2 [265] spectra, MS^3 [265 → 247] spectra).

18 Da less than M11 or M12. Both M13 and M14 produced prominent product ions at m/z 249 by the loss of an H_2O fragment from the parent ions. MS^3 spectral data showed that the daughter ions at m/z 249 continued to lose another CO moiety to form the product ions at m/z 221. After comparing MS^2 and MS^3 spectral data of M13 and M14 with those of M11 and M12, we conclude that M13 and M14 were formed through the respective fragmentation pathways (shown in Fig. 11). From the fragment pathways and characteristic product ions, we inferred that M13 and M14 were also the hydroxylated isomers produced from M11 and M12, which were the isomers and both of them had parent ions at m/z 249.

M15, which eluted at 17.47 min, gave rise to the protonated molecule [M+H]$^+$ at m/z 265, which was 16 Da higher than that of the molecular ion [M+H]$^+$ at m/z 249. The fragment ions at m/z 247 were formed via the elimination of H_2O from the parent ion. The fragment ion at m/z 237 was produced through the loss of CO from the parent ion (shown in Fig. 11). M15 had the characteristic fragment ion series of M12 and TS. M15 was tentatively elucidated as the hydroxylated metabolite of the protonated molecule [M+H]$^+$ at m/z 249, M12.
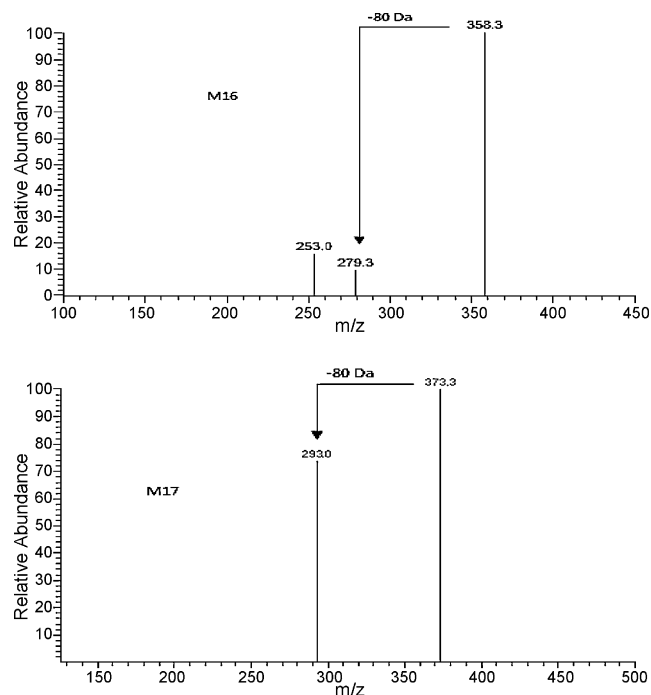
3.2.3. Phase II metabolites of dihydrotanshinone I and tanshinone I

Following the extraction of the rat bile samples with ethyl acetate, the aqueous layers were treated with methanol for protein precipitation and then lyophilized. The residual material was dissolved in the mobile phase, filtered using a 0.22 μm filter and then analyzed by the LC–MS/MS method. O-sulfated conjugated metabolites were detected by ESI-MS in the negative ion mode in the aqueous layers. Neutral loss scan in the MS/MS mode was used to screen the proposed phase II metabolites such as the sulfated products with 80 Da. Based on the above method, two phase II metabolites were observed; the extracted ion chromatograms of M16 and M17 are shown in Fig. 3.

M16 was observed as a sulfate conjugated metabolite of dihydrotanshinone I, which was eluted at 2.37 min and gave rise to the parent [M−H]$^-$ ion at m/z 359. The MS/MS spectrum showed a product ion at m/z 279 corresponding to a neutral loss of 80 Da from the parent [M−H]$^-$ ion at m/z 359 (seen in Fig. 12). The product ion at m/z 253 was produced via the loss of the fragment ion –CH=CH– from the product ion at m/z 279. The product [M−H]$^-$ ion at m/z 279 formed a semiquinone product of DT in the C-ring by hydrogenation of DT quinone, and the monohydroxylated middle-stage product was produced first to provide the hydroxyl group which served as the conjugation site of the sulfate [21]. As such, M16 may represent the DT semiquinone sulfate conjugates and there is the possibility of the position isomers.

M17 was observed as another sulfated metabolite with a retention time of 2.36 min, which gave rise to the parent ion [M−H]$^-$ at m/z 373. The MS/MS spectrum showed a product [M−H]$^-$ ion at m/z 293 corresponding to the neutral loss of 80 Da (seen in Fig. 12). To conjugate with sulfate, DT was biotransformed initially into a monohydroxylated metabolite that could be conjugated with a sulfate moiety. The product ion [M−H]$^-$ at m/z 293 was formed by the monohydroxylation of DT. Therefore, M17 probably represents the O-sulfated metabolite of the monohydroxylated dihydrotanshinone I.
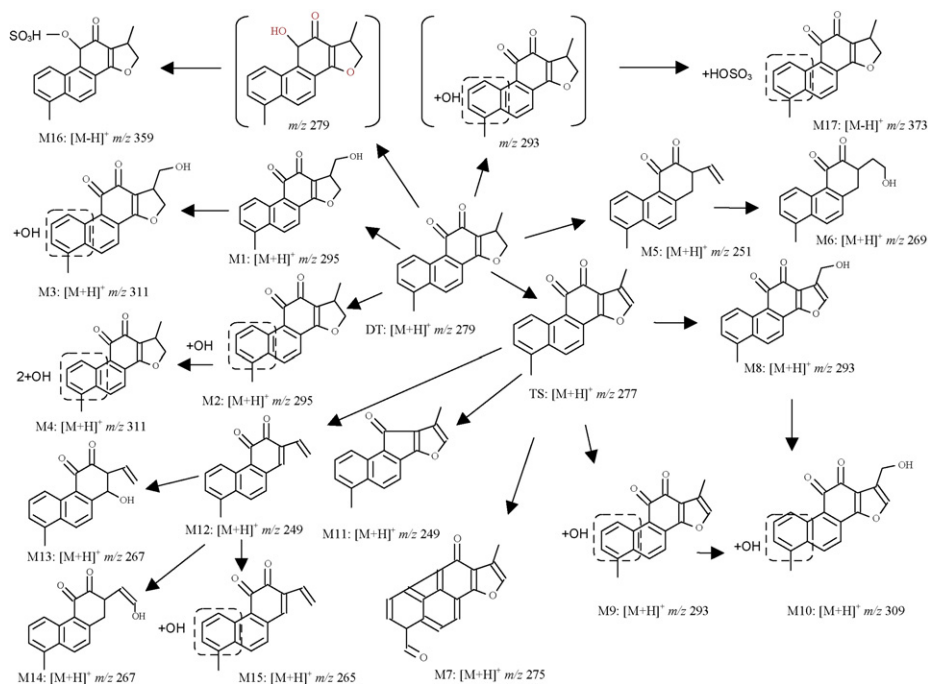
Fig. 13. Proposed biotransformation pathways of tanshinone I and dihydrotanshinone I in rats.

4. Conclusion

This investigation described the application of an LC–ESI-MS method using the positive/negative ion mode and collision induced dissociation to elucidate and identify the metabolites of tanshinone I and dihydrotanshinone I. The structures and fragment pathways of fifteen phase I metabolites and two phase II metabolites in rats were elucidated and analyzed (Fig. 13). The data indicate that the main metabolic pathway of tanshinone I and dihydrotanshinone I can be divided into four categories: the dehydrogenation, hydroxylation, furan ring cleavage and side chain oxidation, and the O-sulfate conjugated reaction. In vivo, dihydrotanshinone I is initially biotransformed into tanshinone I and both dihydrotanshinone I and tanshinone I share similar metabolic pathways. This study provides the valuable and new information on the tanshinone metabolism which is essential for understanding the safety and efficacy of these drugs as well as for the development of novel drug.

References

[1] T.H. Xue, R. Roy, Science 300 (2003) 740.
[2] J. Sun, S.H. Huang, B.K. Tan, M. Whiteman, Y.C. Zhu, Y.J. Wu, Y. Ng, W. Duan, Y.Z. Zhu, Life Sci. 76 (2005) 2849.
[3] J. Ye, H. Duan, X. Yang, W. Yan, X. Zheng, Planta Med. 67 (2001) 766.
[4] M. Yang, A.H. Liu, S.H. Guan, J.H. Sun, M. Xu, D.A. Guo, Rapid Commun. Mass Spectrom. 20 (2006) 1266.
[5] M. Xue, Y.B. Shi, Y. Cui, H.Q. Wang, B. Zhang, Y.J. Luo, Z.T. Zhou, W.J. Xia, R.C. Zhao, H.Q. Wang, Nat. Prod. Res. Dev. 12 (2000) 27.
[6] M. Xue, Y. Cui, H.Q. Wang, Y.B. Shi, B. Zhang, Y.J. Luo, Z.T. Zhou, W.J. Xia, R.C. Zhao, Chin. J. Vet. Drug 33 (1999) 15.
[7] Q.N. Fang, P.L. Zhang, Z.P. Xu, Acta Chem. Sin. 34 (1976) 197.
[8] S.Y. Kim, T.C. Moon, H.W. Chang, Phytother. Res. 16 (2002) 616.
[9] Y.G. Gao, Y.M. Song, Y.Y. Yang, W.F. Liu, J.X. Tang, Acta Pharmacol. Sin. 14 (1979) 75.
[10] E.H. Cao, X.Q. Liu, J.F. Li, Acta Biophys. Sin. 12 (1996) 339.
[11] X.M. Hu, M.M. Zhou, M.X. Hu, J. Wang, F.D. Zeng, Chin. Pharmacol. Bull. 22 (2006) 436.
[12] M.A. Mosaddik, Phytomedicine 10 (2003) 682.
[13] J.Y. Kim, K.M. Kim, J.X. Nan, Pharmacol. Toxicol. 92 (2003) 195.
[14] H.B. Li, F.J. Chen, J. Chromatogr. A 925 (2001) 109.
[15] G. Tian, T. Zhang, Y. Zhang, J. Chromatogr. A 945 (2002) 281.
[16] Z. Shi, J. He, T. Yao, J. Pharm. Biomed. Anal. 37 (2005) 481.
[17] L.M. Zhou, M. Chow, Z. Zuo, J. Pharm. Biomed. Anal. 41 (2006) 744.
[18] J.H. Sun, M. Yang, X.M. Wang, M. Xu, A.H. Liu, D.A. Guo, J. Pharm. Biomed. Anal. 44 (2007) 564.
[19] J.H. Sun, M. Yang, J. Han, B.R. Wang, X.C. Ma, M. Xu, P. Liu, D.A. Guo, Rapid Commun. Mass Spectrom. 21 (2007) 2211.
[20] J. Liu, J.L. Wu, X.R. Wang, Z.W. Cai, Rapid Commun. Mass Spectrom. 21 (2007) 2992.
[21] H.X. Dai, M.M. Wang, X.R. Li, L.J. Wang, Y.H. Li, M. Xue, J. Pharm. Biomed. Anal. 48 (2008) 885.